

Numerical Simulation of Two-phase Flow in Natural Fractured Reservoirs Using Dual Porosity Method on Parallel Computers

Lihua Shen, Tao Cui, Hui Liu, Zhouyuan Zhu, He Zhong, Zhangxin Chen,
Bo Yang, Ruijian He, Huaqing Liu

Abstract

The two-phase oil-water flow in natural fractured reservoirs and its numerical methods are introduced in this paper, where the fracture is modeled by the dual porosity method. Efficient numerical method, including the finite difference method, inexact Newton method nonlinear solver, CPR-FPF preconditioners for linear systems and effective decoupling method, are presented. Parallel computing techniques employed in simulation are also presented. Using those numerical methods and parallel techniques, a parallel reservoir simulator is developed, which is capable of simulating large-scale reservoir models. The numerical results show that our simulator is accurate and scalable compared to the commercial software, and the numerical methods are also effective.

keywords: Reservoir simulation, Oil-water, Two-phase, Dual porosity, Fracture, Parallel computing

1 Introduction

Reservoir simulations are important tools for petroleum engineering, which have been applied to model underground flows and interactions between reservoirs and wells to predict the well performance such as oil rates, water rates and bottom hole pressure. When a reservoir model is large enough, it may take several days or even longer for the simulator to complete a single model. Therefore, the numerical methods and parallel techniques are essential to accelerate the simulations.

As a type of unconventional reservoirs, the reservoir with natural fractures and hydraulic fractures which are commonly seen in tight and shale oil and gas reservoir, the dual-porosity/dual-permeability model and the multiple iteration continua (MINC) model [19, 30] homogenize the fractures and use superpositioned cells to represent the fractures and the matrix. The multiple continuum approaches have been successfully employed in the unconventional reservoir problems. Wu et al. [28, 29] regarded the fractured vuggy rocks as a triple- or multiple-continuum medium with highly permeability and well-connected fractures, low-permeability rock matrix and various-sized vugs. Wu et al. also developed a hybrid multiple-continuum-medium modeling approach to describe different types of fractures including hydraulic fractures, natural fracture network and micro fractures [27]. Jiang and Moinfar and their collaborators designed explicit fracture models coupled with MINC model to simulate the unconventional reservoirs [17, 10]. In reference [31], the authors presented a unified framework model to incorporate the known mechanisms and processes including gas adsorption and desorption, geomechanics effect, Klinkenberg or gas-slippage effect and non-Darcy flow. They also used a hybrid fracture-modeling approach to simulate the unconventional gas reservoirs. Jiang and Younis developed two alternative hybrid approaches to capture the effects of the multiscale fracture systems by combining the advantages of the multi-continuum and discrete-fracture/matrix representations [11].

The numerical methods for reservoir simulations have been explored by both mathematicians and engineers for decades. Killough et al. [12] studied local refinement techniques to improve the accuracy and reduce computational cost comparing to the global grid refinement. Those local refinement techniques are useful for the complex models such as in-situ combustion. Dogru and his group [7] developed parallel simulators using structured and unstructured grids to handle faults, pinchouts, complex wells, polymer flooding in non-fractured and fractured reservoirs. Zhang et al. developed a general-purpose parallel platform for large-scale scientific applications which was designed using the adaptive element methods and the adaptive finite volume methods [32, 33]. It has been applied to black oil simulation using discontinuous Galerkin methods [21]. Chen et al. studied finite element methods and finite difference methods for black oil, compositional and thermal models [6]. They studied Newton methods, linear solvers and preconditioners as well. Chen and his collaborators also developed a parallel platform to support the new-generation simulator development, such as black oil, compositional, thermal, polymer flooding models [16, 22, 23].

Wheeler studied discretization methods, linear solvers, preconditioner techniques and developed a parallel black oil simulator [26]. For the linear solver and preconditioners, many preconditioning methods have been proposed and applied to reservoir simulations such as constrained pressure residual (CPR) methods [14, 3], multi-stage methods [1], multiple level preconditioners [24], fast auxiliary space preconditioners (FASP) [9] and a family of parallel CPR-like methods[14].

In this paper, we present the mathematical model of the dual-porosity reservoirs. After that, we give the numerical methods used in our simulation including the nonlinear solvers, the preconditioner and the linear solver and the parallel technique. Finally, we show the numerical results obtained from our simulator.

2 Mathematical Model

Darcy's law describes the flow of a fluid through porous media, establishing the relationship between the volumetric flow rate and the pressure gradient:

$$Q = -\frac{KA\Delta p}{\mu L} \quad (1)$$

where K is the permeability of a given reservoir, A is the area in the flow direction, Δp is the pressure difference, μ is the viscosity of the fluid and L is the length of the reservoir. In three dimensional space, its differential form is

$$q = \frac{Q}{A} = -\frac{K\nabla p}{\mu} \quad (2)$$

Combining Darcy's law and the mass conservation law for oil and water components, the two-phase model is as follows:

$$\begin{cases} \frac{\partial}{\partial t}(\phi s_o \rho_o) &= \nabla \cdot \left(\frac{K K_{ro} \rho_o}{\mu_o} \nabla \Phi_o \right) + q_o \\ \frac{\partial}{\partial t}(\phi s_w \rho_w) &= \nabla \cdot \left(\frac{K K_{rw} \rho_w}{\mu_w} \nabla \Phi_w \right) + q_w \end{cases} \quad (3)$$

where ϕ and \mathbf{K} are the porosity and the permeabilities (in x -, y - and z -directions) respectively, Φ_α is the potential, s_α , μ_α , $K_{r\alpha}$ and q_α ($\alpha = o, w$) are the saturation, viscosity, relative permeability and production/injection rate, respectively, which satisfy the following constraints:

$$\begin{cases} \Phi_\alpha = p_\alpha - \rho_\alpha g z, \\ s_o + s_w = 1, \\ p_w = p_o - p_{cow}(s_w), \end{cases} \quad (4)$$

where p_α and ρ_α are the pressure and the mass density of phase α ($\alpha = o, w$). p_{cow} is the capillary pressure between oil phase and water phase, g is the gravitational constant and z is the reservoir depth.

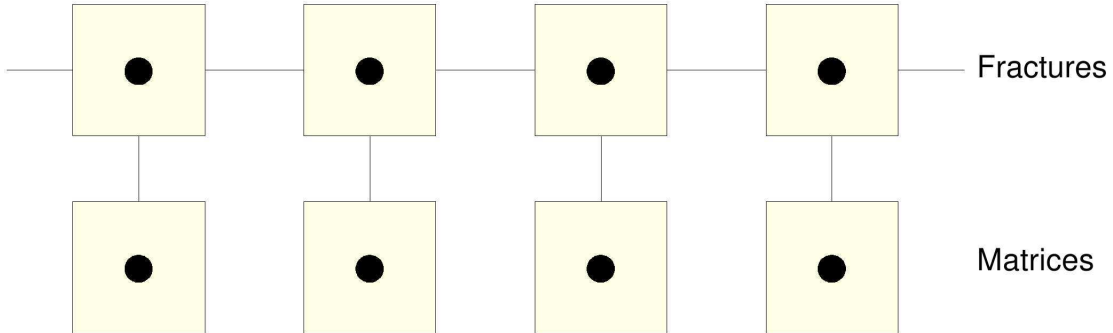


Figure 1: The flow communication for dual porosity model [34]

For the dual-porosity model, fluids can flow between matrix and fracture, as well as fracture and fracture, but there is no flow between matrices. Their flow directions are described by Fig 1. The following equations are used to

describe this model:

$$\begin{cases} \frac{\partial}{\partial t}(\phi_f s_{o,f} \rho_{o,f}) = \nabla \cdot \left(\frac{\mathbf{K}_f K_{r_{o,f}} \rho_{o,f}}{\mu_{o,f}} \nabla \Phi_{o,f} \right) - q_{o,mf} + q_o, \\ \frac{\partial}{\partial t}(\phi_m s_{o,m} \rho_{o,f}) = q_{o,mf}, \\ \frac{\partial}{\partial t}(\phi_f s_{w,f} \rho_{w,f}) = \nabla \cdot \left(\frac{\mathbf{K}_f K_{r_{w,f}} \rho_{w,f}}{\mu_{w,f} b_{w,f}} \nabla \Phi_{w,f} \right) - q_{w,mf} + q_w, \\ \frac{\partial}{\partial t}(\phi_m s_{w,m} \rho_{w,m}) = q_{w,mf} \end{cases} \quad (5)$$

where $(\cdot)_f$ denotes the variables for the fracture and $(\cdot)_m$ for the matrix. Note that here $q_{\alpha,mf} = \omega \left(\frac{K_{r_{\alpha}} \rho_{\alpha,t}}{\mu_{\alpha}} \right)_t (p_f - p_m)$ is a source term which represents the net addition of the fluid to the fracture from the matrix with ω the shape factor. In our simulator, the shape factor we use is based on the work of Warren and Root[25] and Gilman and Kazemi[8]. Note that $(\cdot)_t$ denoted the value at $t = m$ or $t = f$ depending on which is the upstream. The well rate at a perforation, i , is modelled by the sink-source method,

$$q_{\alpha,i} = W_i \frac{\mathbf{K}_f K_{r_{\alpha,f}} \rho_{\alpha,f}}{\mu_{\alpha,f}} (p_b - p), \quad \alpha = o, w \quad (6)$$

where W_i is the well index at the perforation, p_b is the bottom-hole pressure of the well at the perforation, p is the block pressure from oil phase at the perforation. For a producer or an injection well, its well rate is calculated as,

$$q_{\alpha} = \sum_i q_{\alpha,i}, \quad \alpha = o, w. \quad (7)$$

The well index is calculated as follows:

$$W_i = 2\pi * k_h * w_{frac} / (\ln(r_e/r_w) + s). \quad (8)$$

Here k_h is a given value and w_{frac} is the fracture between 0.0 and 1.0 specifying the fraction of a circle that the well models, r_w is the wellbore radius, s is a real number specifying the well skin factor, r_e is the well effective radius calculated from

$$r_e = w_g * \sqrt{A_r / (\pi * w_{frac})} \quad (9)$$

with w_g the geometric factor for the well element, A_r the area perpendicular to the wellbore (e.g., $D_x * D_y$ for a vertical well) and w_{frac} as same above. The other option for the well effective radius is the following Peaceman's form [18]

$$\begin{cases} r_{e,x} = 0.28 \frac{[D_x^2 (\frac{k_y}{k_x})^{1/2} + D_y^2 (\frac{k_x}{k_y})^{1/2}]^{1/2}}{(\frac{k_y}{k_x})^{1/4} + (\frac{k_x}{k_y})^{1/4}}, \\ r_{e,y} = 0.28 \frac{[D_x^2 (\frac{k_z}{k_x})^{1/2} + D_z^2 (\frac{k_x}{k_z})^{1/2}]^{1/2}}{(\frac{k_z}{k_x})^{1/4} + (\frac{k_x}{k_z})^{1/4}}, \\ r_{e,z} = 0.28 \frac{[D_y^2 (\frac{k_z}{k_y})^{1/2} + D_z^2 (\frac{k_y}{k_z})^{1/2}]^{1/2}}{(\frac{k_z}{k_y})^{1/4} + (\frac{k_y}{k_z})^{1/4}}, \end{cases} \quad (10)$$

where $r_{e,x}$, $r_{e,y}$ and $r_{e,z}$ are the well effective radius in x , y and z direction respectively, D_x , D_y and D_z are the block sizes in x , y and z direction respectively, k_x , k_y and k_z are the permeabilities in x , y and z direction respectively.

3 Numerical Methods and Parallel Computing

In this paper, the fully implicit method (FIM) is applied, and the oil phase pressure p , water saturation s_w and the well bottom hole pressure p_b are unknowns. For the time differential and the space differential term, we use the backward Euler scheme and cell-centered finite difference method as discretization methods.

The system is highly nonlinear,

$$F(x) = 0 \quad (11)$$

where F is a nonlinear map from \mathcal{R}^N to \mathcal{R}^N with $N = 2 \times n + \tau$. Here n is the number of grid blocks and τ is the well size. In this nonlinear equation, the properties related to the saturation are strongly nonlinear while the properties related to the pressure are weakly nonlinear. In our simulation, we use Newton method (or inexact Newton method) to solve it.

3.1 Nonlinear Solver

The inexact Newton method can be regarded as an extension of the standard Newton method. Let A be the Jacobian matrix of $F(x)$ and y is the correction between the last step approximate solution and the current step one. Its algorithm [5] is as follows:

Algorithm 1 The Inexact Newton Method

- 1: Given an initial guess x^0 and a termination tolerance ϵ , let $l = 0$ and assemble the right-hand side b .
- 2: **while** $\|b\| \geq \epsilon$ **do**
- 3: Compute the Jacobian matrix A .
- 4: Determine η_l .
- 5: Find a solution y such that

$$\|Ay - b\| \leq \eta_l \|b\|, \quad (12)$$

- 6: Let $l = l + 1$ and $x^l = x^{l-1} + y$.
 - 7: Compute the new right-hand side b
 - 8: **end while**
 - 9: $x^* = x^l$ is the approximate solution of the nonlinear system, $F(x) = 0$.
-

We can see that the algorithm is the same as Newton method except the choice of the tolerance θ . The standard Newton method usually applies a small constant such as $1.0e - 6$, while the **Algorithm 1** uses adaptive θ_l tolerance to avoid over solution. Common methods are defined as follows [5]:

$$\theta_l = \begin{cases} \frac{\|b(x^l) - r^{l-1}\|}{\|b(x^{l-1})\|}, \\ \frac{\|b(x^l)\| - \|r^{l-1}\|}{\|b(x^{l-1})\|}, \\ \gamma \left(\frac{\|b(x^l)\|}{\|b(x^{l-1})\|} \right)^\beta, \quad \gamma \in [0, 1], \quad \beta \in (1, 2] \end{cases} \quad (13)$$

where r^l is the residual of the l -th iteration.

3.2 Preconditioner and Linear Solver

For each Newton iteration, we need to solve a linear system $Ax = b$ which is very time consuming. To improve the efficiency, we choose a proper preconditioner, CPR-FPF method [14], for the model. Each grid block has four unknowns, pressures (p_f and p_m) and saturations ($s_{w,f}$ and $s_{w,m}$) for matrix and fracture, and four equations. In our linear system, each unknown and each row are arranged cell by cell, in this case, the Jacobian matrix is a block matrix. It is also well-known that block matrix has better convergence than point-wise matrix.

Before solving the linear system $Ax = b$, a decoupling operation D is applied, and an equivalent system is obtained:

$$D^{-1}Ax = D^{-1}b. \quad (14)$$

A proper decoupling method can improve linear solver dramatically. Many decoupling strategies have been proposed, such as Quasi-IMPES[13] method and ABF[2] method. In this paper, a modified Gauss-Jordan elimination method is applied.

3.3 Parallel Computing

The simulator is based on our parallel platform PRSI [16], which is developed using C language and MPI (Message Passing Interface). The platform has implemented many modules, such as grid generation, load balancing, well management, parallel input and output, distributed matrix and vector, linear solver and preconditioner, communication management and visualization. Based on the platform, physical modules, such as rock properties and rock-fluid properties, are implemented. More details can be read from reference [16].

4 Numerical Results

Example 1 The grid dimension is $10 \times 10 \times 1$ with sizes 102.04 ft. in x and y directions and 100.0 ft. in z direction from top to bottom. The depth of the top layer center is 2000.0 ft. The permeabilities for the matrix in x , y and z directions are 100, 100, 10 mD respectively. The permeability for the fracture in x , y and z directions are 395.85 mD. The reference porosity for the matrix is 0.1392. The reference porosity for the fracture is 0.039585. The rock compressibilities for the matrix and fracture are both $3e-06$ (1/psi). The reference pressure is 15.0 psi for both the matrix and the fracture. Component properties: densities of oil and water are 58.0 lbm/ft³ and 62.4 lbm/ft³ respectively. The reference pressure is 15 psi at which the oil formation volume factor is 1.036 RB/STB and the oil viscosity is 40.0 cp. The oil compressibility is const $1.313e-5$ l/psi. The initial conditions are as follows: initial pressure for the matrix is 2000 psi, initial pressure for the fracture is 1980 psi, and initial water saturations are 0.08 and 0.01 in matrix and fracture respectively. There are one injection well and two production wells. All of them are vertical. Injection well has maximum water injection rate 500.0 bbl/day, maximum bottom hole pressure $5.0e+4$ psi, well index 200.0 with perforation at cell [5 1 1]. Both of the production well has maximum oil production rate 300.0 STB/day, minimum bottom hole pressure 15 psi with well radius 0.25ft. The perforation of Producer 1 is at cell [1 10 1] while the perforation of Producer 2 is at cell [10 10 1]. The simulation period is 800 days.

The results of oil production rate, bottom-hole-pressure and water rate are shown in Fig. 2, 3, 4, from which we can see that the results from our simulator and from CMG IMEX match very well. This proves our methods and implementation are correct.

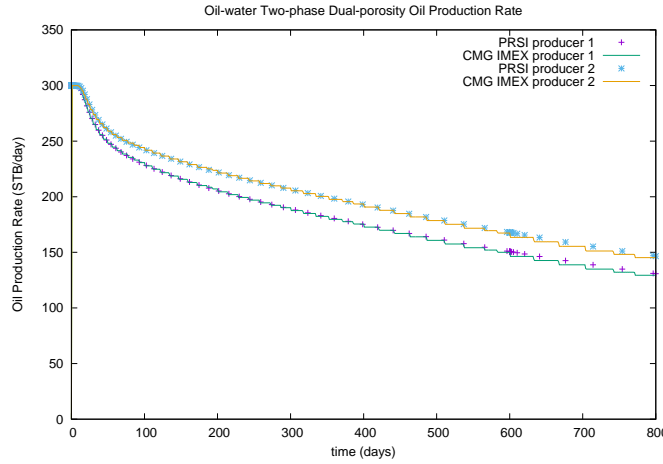


Figure 2: Example 1: Oil production rate (unit: STB/day).

Example 2 The grid dimension is $10 \times 10 \times 3$ with mesh size 102 ft. in x and y directions and 100.0 ft. in z direction from top to bottom. The depth of the top layer center is 2000.0 ft. The permeabilities for the matrix in x , y and z directions are 100, 100, 100 mD respectively. The permeability for the fracture in x , y and z directions are 395.85 mD. The reference porosity for the matrix is 0.1392. The reference porosity for the fracture is 0.039585. The rock compressibilities for the matrix and fracture are both $3e-06$ (1/psi). The reference pressure is 15.0 for both the matrix and the fracture. Component properties: densities of oil and water are 58.0 lbm/ft³ and 62.4 lbm/ft³ respectively. PVT: the reference pressure is 15 psi at which the oil formation volume factor is 1.036 RB/STB and the

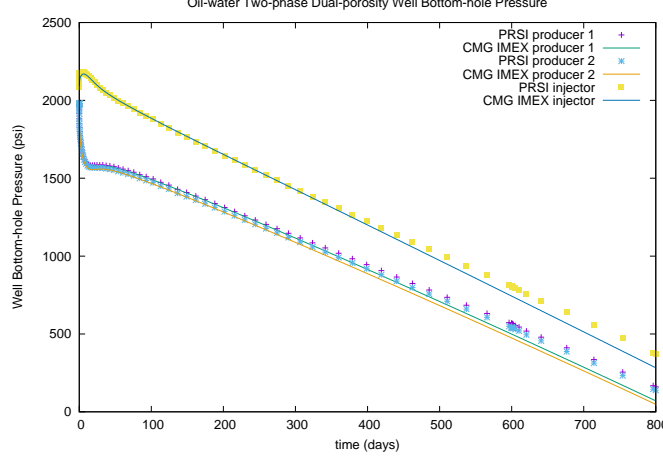


Figure 3: Example 1: Well bottom-hole pressure (pressure unit: psi).

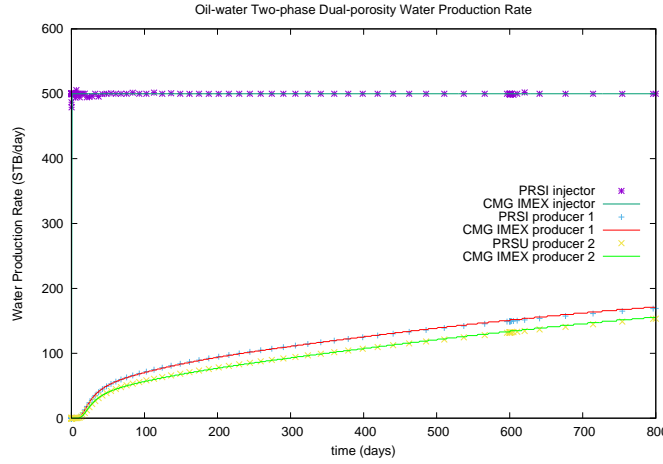


Figure 4: Example 1: Water rate (unit: STB/day).

oil viscosity is 40.0 cp. The oil compressibility is const $1.313e-5$ l/psi. The initial conditions are as follows: initial pressure for the matrix is 800 psi, initial pressure for the fracture is 500 psi, and initial water saturations are 0.08 and 0.01 in matrix and fracture respectively. There are one injection well and two production wells. All of them are vertical. Injection well has maximum water injection rate 200.0 bbl/day, maximum bottom hole pressure $5.0e+4$ psi, well index 200.0 with perforation at cell [5 5 1]. Both of the production well has maximum oil production rate 500.0 STB/day, minimum bottom hole pressure 15 psi with well radius 0.25ft. The perforation of Producer 1 is at cell [1 1 1] while the perforation of Producer 2 is at cell [10 10 1]. The simulation period is 1600 days.

The results of oil production rate, bottom-hole-pressure and water rate are shown in Fig. 5, 6, 7. Again, these figures show that our simulator match CMG simulator.

Example 3 This example tests the scalability of our two-phase dual porosity simulator by computing Example 1 with grid dimension $500 \times 500 \times 50$.

As we introduced before, we employ the GMRES linear solver and CPR preconditioner. Table 4 shows the numerical summaries, which show that our numerical methods are stable when increasing CPU cores. Figure 8 presents the scalability of our simulator, which demonstrates that the simulator and parallel implementation are scalable.

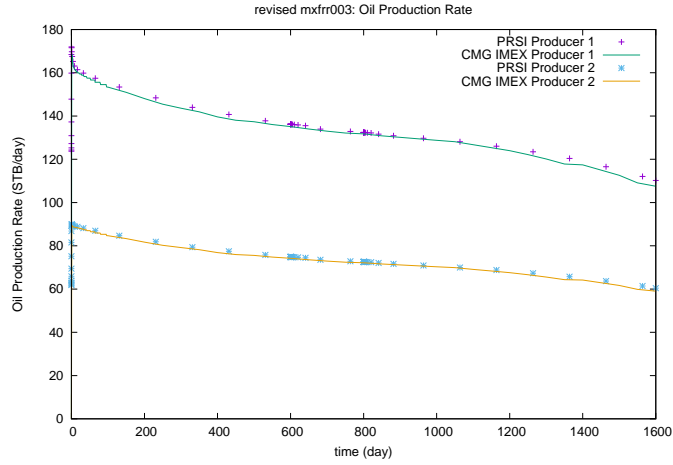


Figure 5: Example 2: Oil production rate (unit: STB/day).

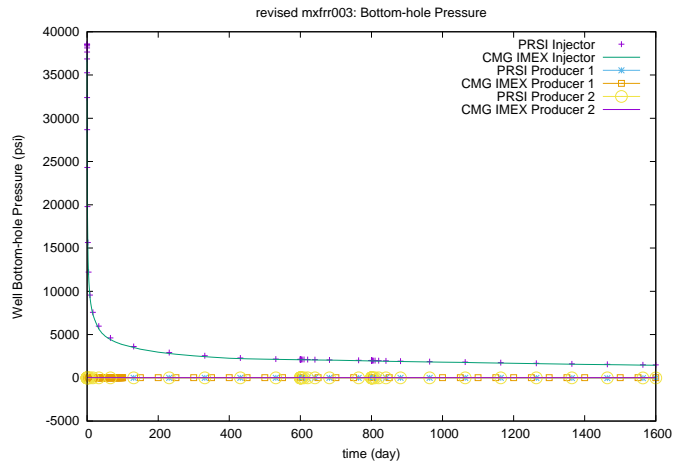


Figure 6: Example 2: Well bottom-hole pressure (pressure unit: psi).

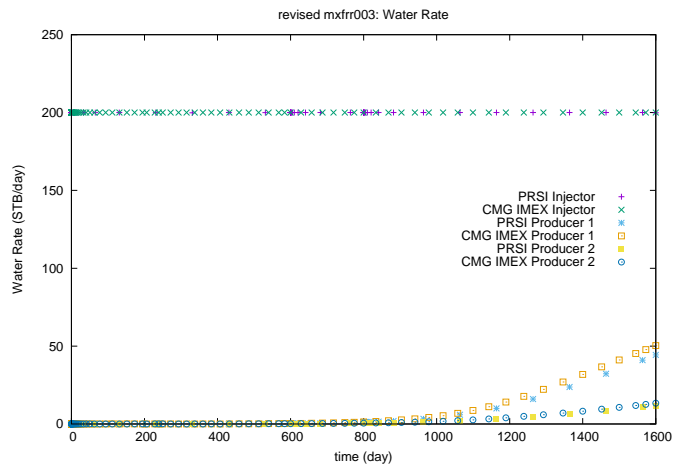


Figure 7: Example 2: Water rate (unit: STB/day).

#MPIs	8	64
#Time steps	68	68
#Newton iterations	273	267
#total linear iterations	641	623
#total running time(s)	20009.71	2531.91

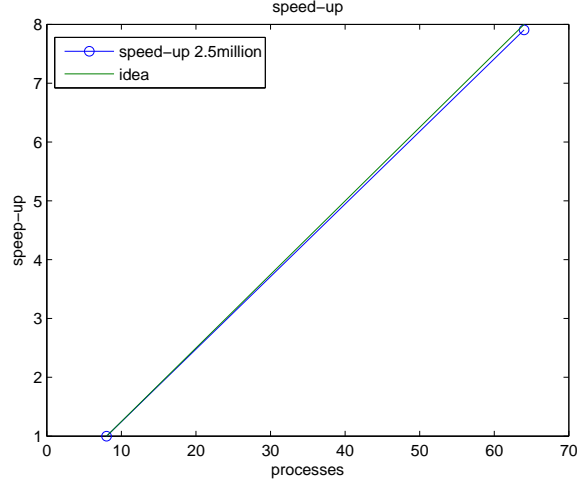


Figure 8: Example 3: speed-up.

5 Conclusion

This paper presents our work on development of two-phase oil-water simulator for natural fractured reservoirs using dual porosity method. Effective numerical methods and parallel computing techniques are introduced. From the numerical experiments, we can see that our results match commercial simulator, CMG IMEX, and the simulator has good parallel scalability and is capable of handling large scale reservoir simulation problems.

6 Acknowledgements

This work is partially supported by Department of Chemical Petroleum Engineering, University of Calgary, NSERC, AIEES, Foundation CMG, AITF iCore, IBM Thomas J. Watson Research Center, Frank and Sarah Meyer FCMG Collaboration Center, WestGrid (www.westgrid.ca), SciNet (www.scinetc.ca) and Compute Canada Calcul Canada (www.computeCanada.ca).

References

- [1] T. Al-Shaalan, H. Klie, A. Dogru, and M. Wheeler, Studies of robust two stage preconditioners for the solution of fully implicit multiphase flow problems, SPE Reservoir Simulation Symposium, 2009.
- [2] R. Bank, T. Chan, W. Coughran Jr., and R. Smith, The Alternate-Block-Factorization procedure for systems of partial differential equations, BIT Numerical Mathematics, 29(4), 1989, 938-954.
- [3] H. Cao, T. Schlumberger, A. Hamdi, J. Wallis, and H. Yardumian, Parallel scalable unstructured CPR-type linear solver for reservoir simulation, SPE Annual Technical Conference and Exhibition, 2005.
- [4] X. Cai and M. Sarkis, A restricted additive Schwarz preconditioner for general sparse linear systems, SIAM Journal on Scientific Computing, 21(2), 1999, 792-797.

- [5] T. Chen, N. Gewecke, Z. Li, A. Rubiano, R. Shuttleworth B. Yong and X. Zhong, Fast Computational Methods for Reservoir Flow Models, 2009.
- [6] Z. Chen, G. Huan and Y. Ma, Computational methods for multiphase flows in porous media, Vol. 2, Siam, 2006.
- [7] A. Dogru, L. Fung, U. Middy, T. Al-Shaalan, and J. Pita, A next-generation parallel reservoir simulation for the giant reservoirs, SPE/EAGE Reservoir Characterization & Simulation Conference, 2009.
- [8] J.R. Gilman and H. Kazemi, Improvements in Simulation of Naturally Fractured Reservoirs, SPE-10511-PA, Vol. 23(04), 1983, 695-707.
- [9] X. Hu, W. Liu, G. Qin, J. Xu, and Z. Zhang, Development of a fast auxiliary subspace pre-conditioner for numerical reservoir simulators, SPE Reservoir Characterisation and Simulation Conference and Exhibition, 2011.
- [10] J. Jiang, Y. Shao, R. M. Younis, et al., Development of a multi-continuum multi-component model for enhanced gas recovery and CO₂ storage in fractured shale gas reservoirs, SPE Improved Oil Recovery Symposium, Society of Petroleum Engineers, 2014.
- [11] J. Jiang, R. Younis, et al., Hybrid coupled discrete-fracture/matrix and multi-continuum models for unconventional-reservoir simulation, SPE Journal 21(03), 2016 1009-1027.
- [12] J. Killough, D. Camilleri, B. Darlow, and J. Foster, Parallel reservoir simulation based on local grid refinement. SPE-37978, SPE Reservoir Simulation Symposium., Dallas, 1997.
- [13] S. Lacroix, Y. Vassilevski, and M. Wheeler, Decoupling preconditioners in the implicit parallel accurate reservoir simulation (IPARS), Numerical linear algebra with applications, 8(8), 2001, 537-549.
- [14] H. Liu, K. Wang, and Z. Chen, A family of constrained pressure residual preconditioners for parallel reservoir simulations, Numerical Linear Algebra with Applications, Vol. 23(1), 2016, 120-146.
- [15] H. Liu, Dynamic load balancing on adaptive unstructured meshes, 10th IEEE International Conference on High Performance Computing and Communications, 2008.
- [16] H. Liu, K. Wang, Z. Chen, K. Jordan, J. Luo, and H. Deng, A parallel framework for reservoir simulators on distributed-memory supercomputers, SPE-17645-MS, SPE/IATMI Asia Pacific Oil & Gas Conference and Exhibition, 20-22 October, Nusa Dua, Bali, Indonesia, 2015.
- [17] A. Moynfar, A. Varavei, K. Sepehrnoori, R. T. Johns, et al., Development of a coupled dual continuum and discrete fracture model for the simulation of unconventional reservoirs, SPE Reservoir Simulation Symposium, Society of Petroleum Engineers, 2013.
- [18] Peaceman, D. W., Interpretation of Well-Block Pressures in Numerical Reservoir Simulation with Non-Square Grid Blocks and Anisotropic Permeability, SPE Journal, 23(3), 1983, 531-543.
- [19] K. Pruess, et al. A practical method for modeling fluid and heat flow in fractured porous media, Society of Petroleum Engineers Journal, Vol. 25(01), 14-26 1985.
- [20] J. Wallis, R. Kendall, and T. Little, Constrained residual acceleration of conjugate residual methods, SPE Reservoir Simulation Symposium, 1985.
- [21] K. Wang, L. Zhang, Z. Chen, Development of discontinuous Galerkin methods and a parallel simulator for reservoir simulation, SPE-176168-MS, SPE/IATMI Asia Pacific Oil & Gas Conference and Exhibition, 20-22 October, Nusa Dua, Bali, Indonesia, 2015.
- [22] K. Wang, H. Liu, and Z. Chen, A scalable parallel black oil simulator on distributed memory parallel computers, Journal of Computational Physics, Vol. 301, 19-34.
- [23] K. Wang, H. Liu, J. Luo, and Z. Chen, Parallel simulation of full-field polymer flooding, The 2nd IEEE International Conference on High Performance and Smart Computing, 2016.

- [24] B. Wang, S. Wu, Q. Li, H. Li, C. Zhang, and J. Xu, A multilevel preconditioner and its shared memory implementation for new generation reservoir simulation, SPE-172988-MS, SPE Large Scale Computing and Big Data Challenges in Reservoir Simulation Conference and Exhibition, 15-17 September, Istanbul, Turkey, 2014.
- [25] J.E. Warren and P.J. Root, The Behavior of Naturally Fractured Reservoirs, SPE-426-PA, Vol. 3(02), 1963. 245-255.
- [26] M. Wheeler, Advanced techniques and algorithms for reservoir simulation, II: The multiblock approach in the integrated parallel accurate reservoir simulation (IPARS), the IMA Volumes in Mathematics and its Applications, Springer New York, 9-19, 2002.
- [27] Y.S. Wu, N. Li, C. Wang, Q. Ran, J. Li, J. Yuan, et al., A multiple-continuum model for simulation of gas production from shale gas reservoirs, SPE Reservoir Characterization and Simulation Conference and Exhibition, Society of Petroleum Engineers, 2013.
- [28] Y.S. Wu, G. Qin, R.E. Ewing, Y. Efendiev, Z. Kang, Y. Ren, et al., A multiple-continuum approach for modeling multiphase flow in naturally fractured vuggy petroleum reservoirs: International Oil & Gas Conference and Exhibition in China, Society of Petroleum Engineers, 2006.
- [29] Y.S. Wu, Y. Di, Z. Kang, P. Fakcharoenphol, A multiple-continuum model for simulating single-phase and multiphase flow in naturally fractured vuggy reservoirs, Journal of Petroleum Science and Engineering, 78(1), 2011, 13-22.
- [30] Y.S. Wu, K. Pruess, et al., A multiple-porosity method for simulation of naturally fractured petroleum reservoir, SPE Reservoir Engineering 3(01), 1998, 327-336.
- [31] Y.S. Wu, J. Li, D. Ding, C. Wang, Y. Di, et al., A generalized framework model for the simulation of gas production in unconventional gas reservoirs, SPE Journal 19(05), 2014, 845-857.
- [32] L. Zhang, A parallel algorithm for adaptive local refinement of tetrahedral meshes using bisection, Numer. Math.: Theory, Methods and applications, Vol. 2, 65-89 2009.
- [33] L. Zhang, T. Cui and H. Hui, A set of symmetric quadrature rules on triangles and tetrahedra, J. Comput. Math. 2009, 27(1), 89-96.
- [34] CMG Ltd, IMEX User Guid, Version 2014, 2014.